Supporting Information for "Internal tide surface signature and incoherence in the North Atlantic"

N. Lahaye [1], A. Ponte [2], J. Le Sommer [3], and A. Albert [3]

[1]Odyssey team, Inria & IRMAR, Campus Universitaire de Beaulieu, Rennes, France

[2]Ifremer, Université de Brest, CNRS, IRD, Laboratoire d'Océanographie Physique et Spatiale, IUEM, Brest, France

[3]University Grenoble Alpes, CNRS UMR IGE, Grenoble, France

Contents of this file

Introduction This supporting information presents validation material of the internal tide field in the NEMO-eNATL60 simulation. The validation consists more precisely in a comparison between eNATL60 total and incoherent tidal signals and observations and previously-published model-based results. We recall that a description and assessment of the simulation, and especially of the mesoscale field and barotropic tide, was provided by Brodeau, Le Sommer, and Albert (2020).

Text S1. Figure S1 compares the mode 1 coherent internal tide Sea Level Anomaly (SLA) in eNATL60 and the SLA estimated from satellite altimeters, using HRET v8.1 (Zaron,

2019). HRET data is available at `https://ingria.ceoas.oregonstate.edu/fossil/HRET`. A reasonable agreement is visible, for both the amplitude and the patterns of the internal tide signature. Note that both estimates define the coherent internal tide signal as the harmonic component over a given time window, but the latter is shorter in eNATL60 compared to multi-mission satellite estimates (8 months vs. $\sim$ 25 years). Therefore, the amplitude of the coherent internal tide field is greater in eNATL60, to an extent that seems reasonable in the Figure. Some discrepancies can be observed in the western region of the domain for the S_2 constituent. The potential sources of error are numerous and we are not able to identify a dominant one. It should be noted, however, that the mesoscale activity is elevated in this part of the basin. This could result in the 8-month estimate being less representative of a longer time-window estimate of the coherent tide due to significant variability at timescales longer than 8 months. Conversely, the internal tide signal from altimetry in these regions is challenging to capture due to the strong signature of balanced motions and the high degree of incoherence. This is exemplified by the white regions in the HRET estimates, which correspond to portions of the domain where no significant coherent internal tide signal was retrieved.

Text S2. In Figure S2, we compare the variance of the semidiurnal surface horizontal velocity (*i.e.* the horizontal kinetic energy) between a 1-year long average in eNATL60 (July 2009 to June 2010) and an estimate from the Global Drifter Program (GDP) dataset. The latter, which is based on time filtering in a Lagrangian frame (bandpass filtering at 1.97 ± 0.2 cpd), is converted to an Eulerian estimate using the method proposed by Caspar-Cohen and co-authors (manuscript submitted) and should be interpreted with

caution given some inherent uncertainty. The corresponding data, together with the scripts to compute this estimate, are available at Caspar-Cohen (2024). Note that these diagnostics include the total tidal signal (coherent and incoherent, barotropic plus baroclinic), as we are not able to separate the different contributions from the surface drifters data. The contribution from the barotropic mode is only significant in shallow regions, however. The variance in eNATL60 is smaller than the estimate from the GDP, particularly in the region of the Gulf Stream and the North Atlantic Current. Although we do not have a straightforward explanation for this, it should be noted that these regions correspond to a small level of energy. Another area of low energy in eNATL60 compared to GDP is visible off the Amazon shelf, which may be due to some generation of IT that is not included in the eNATL60 simulation due to domain restriction. In contrast, the internal tide appears to be more energetic in eNATL60 than in the GDP-based estimate in the southeastern part of the domain. There are also discrepancies visible near coastal shelves or other abrupt topography, where the spatial binning becomes coarse compared to the variations of depths, making the drifter estimates less reliable. However, there is a reasonable agreement overall, particularly regarding the patterns and hot spots of semidiurnal kinetic energy.

Text S3. Figure S3 shows the RMS amplitude of incoherent and total baroclinic sea level fluctuations, which can be compared with previously published results, and in particular with the HYCOM simulation discussed by Nelson et al. (2019): the map of total baroclinic SLA can be compared with their Figure 2 and the map of incoherent SLA with their Figure 3. More interestingly, the incoherent variance fraction shown in the Figure can

be compared with Figure 4 of Nelson et al. (2019) and with Figure 9 of Zaron (2017), which is an estimate based on nadir altimeters (also shown in Fig. 4 of Nelson et al. (2019) for comparison). Note that comparison with the latter is limited by the fact that Zaron (2017) includes only the mode 1 (*i.e.* it better compares with our eNATL60 estimate shown in the Figure 3 of the main document), but the difference is moderate because mode 1 contribution is dominant in SLA. Besides, our estimate is based on a 8-month time window for defining the coherent part, while Nelson et al. (2019) used 5 years of simulation, and Zaron (2017) 23 years of satellite data. Nonetheless, the different estimates agree reasonably well: one recognizes the smaller incoherent fraction (typical values around 0.2) in the Eastern part of the domain, except offshore the UK where it is elevated, localized patterns of weaker incoherence along the Caribbean and incoherent beams propagating Northward from the North Brazil coast (with typical values around 0.75).

Text S4. Finally, Figure S3 (lower panels) compares the incoherent variance fraction for the SLA and the surface current, clearly exhibiting the overall larger level of incoherence in the surface velocity compared to SLA, as discussed in the paper. We checked that we obtain qualitatively the same maps (with the same contrast between SLA and surface currents) if we build an estimate based on the average over the modes of the incoherent energy fraction (Fig. 3 in the paper) weighted by the modal contribution to the variance of the corresponding field (see Fig. 2 in the paper, where the RMS amplitude instead of the variance is plotted).

References

Brodeau, L., Le Sommer, J., & Albert, A. (2020). *ocean-next/eNATL60: Material describing the set-up and the assessment of NEMO-eNATL60 simulations.* [Dataset]. Zenodo. doi: 10.5281/zenodo.4032732

Caspar-Cohen, Z. (2024). *Surface drifters and high resolution global simulations mapping of internal tide surface energy.* [Dataset]. Zenodo. doi: 10.5281/zenodo.10851200

Nelson, A. D., Arbic, B. K., Zaron, E. D., Savage, A. C., Richman, J. G., Buijsman, M. C., & Shriver, J. F. (2019, September). Toward Realistic Nonstationarity of Semidiurnal Baroclinic Tides in a Hydrodynamic Model. *J. Geophys. Res. Oceans*, *124*(9), 6632–6642. doi: 10.1029/2018JC014737

Zaron, E. D. (2017, January). Mapping the nonstationary internal tide with satellite altimetry. *J. Geophys. Res. Oceans*, *122*(1), 539–554. doi: 10.1002/2016JC012487

Zaron, E. D. (2019, January). Baroclinic Tidal Sea Level from Exact-Repeat Mission Altimetry. *J. Phys. Oceanogr.*, *49*(1), 193–210. doi: 10.1175/JPO-D-18-0127.1

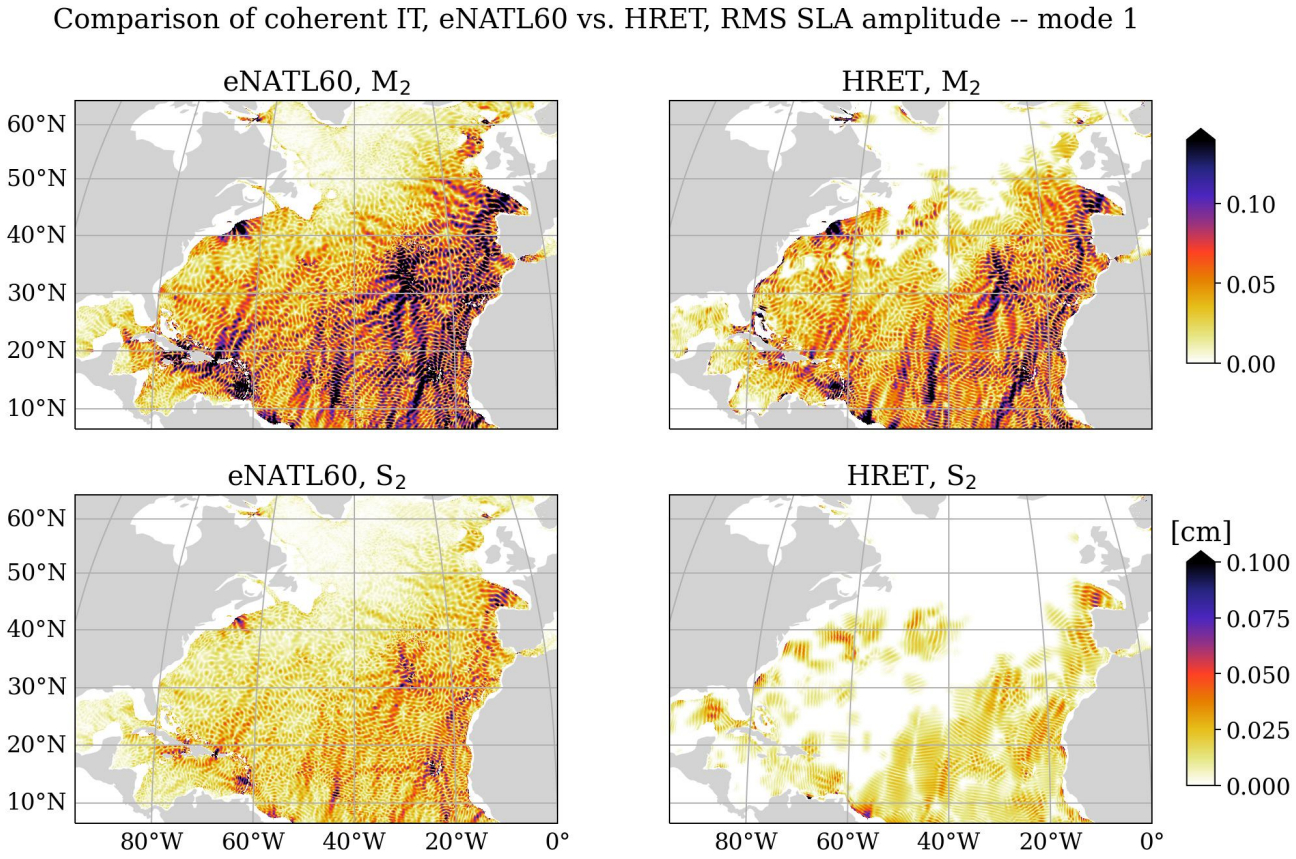

Figure S1. Sea Level Anomaly associated with the coherent part of the first baroclinic mode for the M_2 (top) and S_2 (bottom) constituents, as computed from the eNATL60 run (8-month harmonic fits) and data from satellite altimeters (HRET v8.1).

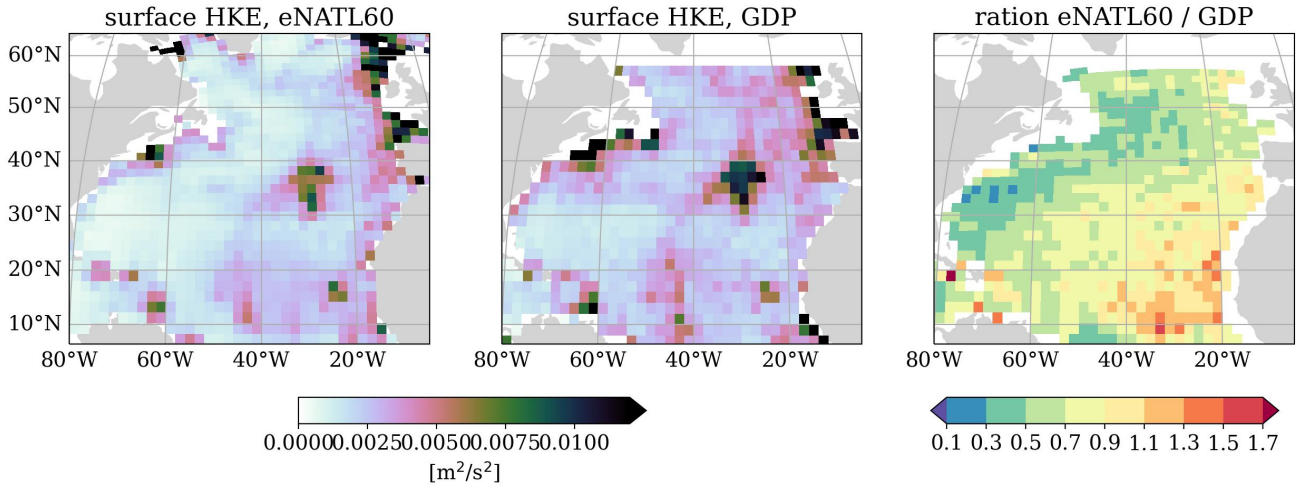

Figure S2. Comparison of the surface horizontal kinetic energy (divided by ρ) in the semidiurnal band computed from eNATL60 run (left panel), and estimated from the GDP dataset (middle panel) and averaged over $\sim 2^\circ$ bins. It includes both the baroclinic and barotropic parts. The right panel shows the ratio of the two estimates, after interpolation on the GDP estimate grid.

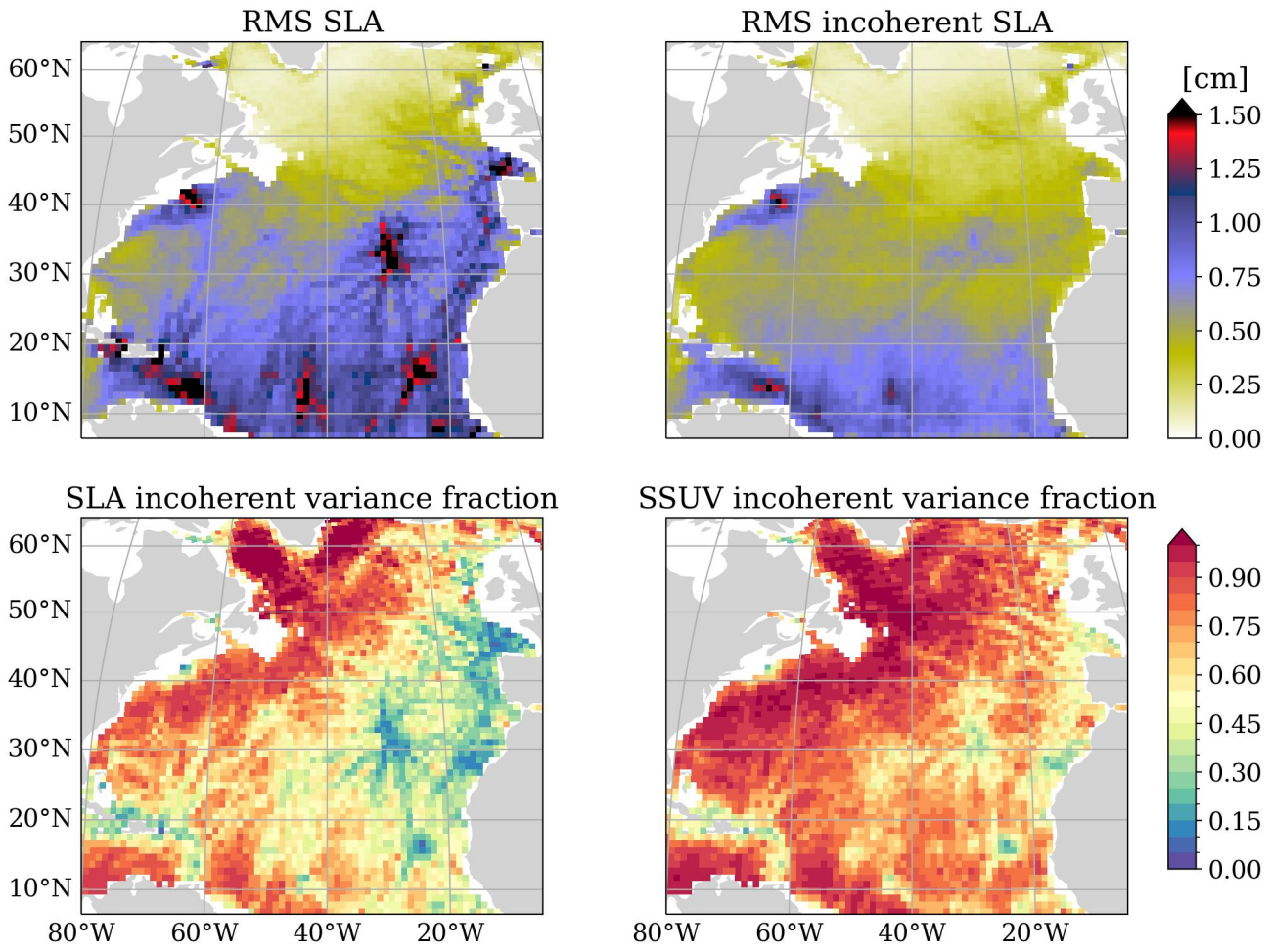

Figure S3. Top: RMS amplitude of the total (left) and incoherent (right) baroclinic Sea Level Anomaly in the semidiurnal band., averaged over $\sim 1°$ spatial bins. Bottom: incoherent variance fraction for the baroclinic Sea Level Anomaly (left) and the baroclinic surface velocity (right). All plots come from the eNATL60 outputs.